A TLE-based Algorithm for Correcting Empirical Model Densities during Geomagnetic Storms

Daniel A. Brandt[1], Charles D. Bussy-Virat[2], Aaron J. Ridley[3]
branddan@umich.edu[1], cbv@umich.edu[2], ridley@umich.edu[3]
Department of Climate and Space Science and Engineering, University of Michigan – Ann Arbor

INTRODUCTION

Thermosphere Dynamics

- Neutral densities increase up to 800% during geomagnetic storms[1].
- Satellite two-line element sets (TLEs) show increased orbital decay during geomagnetic storms from increased drag[2].

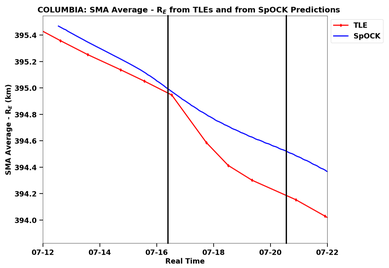

Figure 1: SpOCK inaccurately modeling orbital decay of the Columbia CubeSat during a geomagnetic storm.

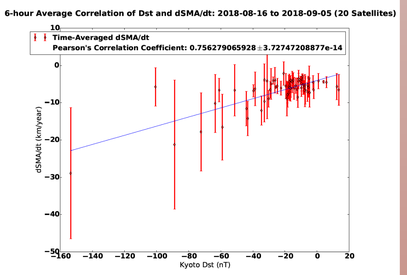

Figure 2: The strongly positive correlation between rate of deorbit and geomagnetic activity indicated by Dst for 20 identical Flock 2K CubeSats.

Weakness of Empirical Atmospheric Models

- Models like NLRMSISE-00 poorly reproduce the storm-time density increase[3].
- Poor model performance reduces accuracy of orbital propagators (Figure 1) like UofM's Spacecraft Orbital Characterization Kit (SpOCK)[4].

Model Correction

- High-Accuracy Satellite Drag Model (HASDM) used by USAF to correct Jacchia-1970[5].
- HASDM Dynamics Calibration Atmosphere (DCA) uses Space Surveillance Network data of >75 orbiting spheres to estimate corrections to F10.7 and a_p[5].
- Doornbos et al. 2008 used TLEs to estimate corrections but assumed TLE-derived densities were sufficient[6].
- We propose a method that estimates corrections by minimizing orbit error between SpOCK orbits and TLEs.

OBJECTIVES

- Develop an algorithm capable of **estimating corrections to empirical model densities** during geomagnetic storms.
- **Validate** the corrected densities returned by the algorithm in comparison to Level 2 densities measured by the SWARM spacecrafts.
- Demonstrate the algorithm's **self-consistency** across a wide variety of modeled spacecraft orbits during different storms.
- Demonstrate the efficacy of using **orbit error minimization** to back out corrected densities from empirical atmospheric models.

METHODOLOGY

Multifaceted Optimization Algorithm:

Corrects NRLMSISE-00 model densities:

1. **Area Optimization Algorithm (AROPT):**
   - Loop over preceding quiet time and adjust cross-sectional area until orbit error is minimized.
   - Obtain the **mean** of the optimized area distribution (assumes NLRMISISE-00 underpredicts effects from storms)
2. **F10.7 Optimization Algorithm (FOPT):**
   - Repeat the loop, adjusting F10.7 until orbit error is minimized; retrieve the F10.7 correction for each interval.
3. **a_p Optimization Algorithm (APOPT):**
   - Hold constant the most recent pre-storm F10.7 adjustment.
   - Loop through the storm, adjusting a_p until orbit error is minimized; retrieve the a_p correction for each interval
4. **Applying Corrections**
   - Linearly interpolate median corrections across all satellites.
   - Apply corrections to F10.7 and Ap inputs to NRLMSISE-00 along the orbits of validation spacecraft.
   - Compare the resulting densities to *in-situ* measurements.

Scenario:

- Time: 2017-05-23 and 2017-06-02
- Calibration Targets: 10 Flock 3P satellites
- Validation Satellites: SWARM-A and -B.

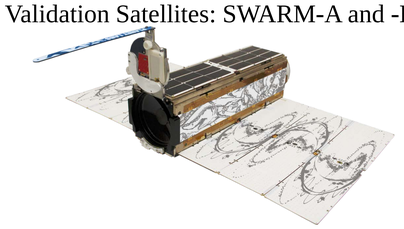

Figure 4: An image of one of the Flock 3P satellites.

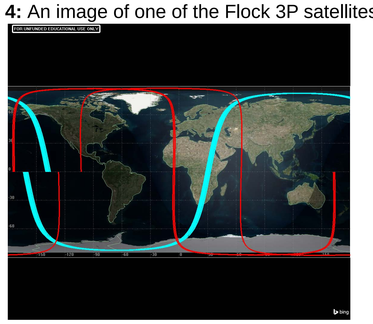

Figure 5: Orbits of the Flock 3P CubeSats (cyan) and of SWARM (red) in the June 2017 storm.

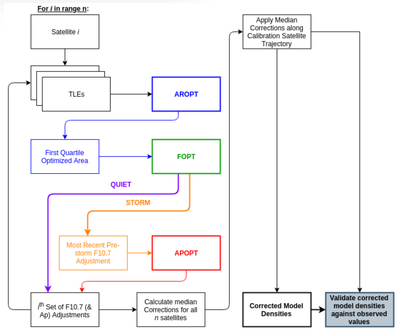

Figure 5: A flowchart of the MOA algorithm. FOPT corrections are held constant during the storm, while APOPT corrections vary.

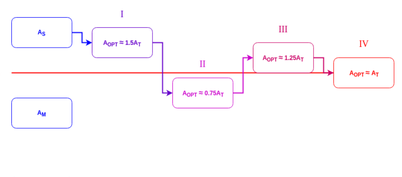

Figure 6: A flowchart of the bracketing processes used by AROPT to find the optimized area.

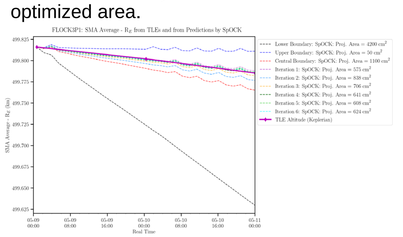

Figure 7: AROPT optimizing the area of the Flock 3P 1 satellite.

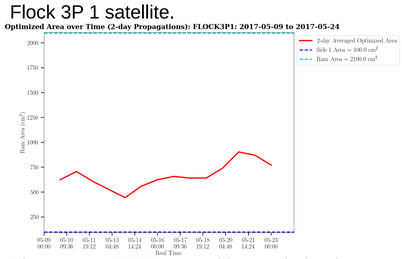

Figure 8: AROPT's resulting optimized areas for Flock 3P 1 during quiet time.

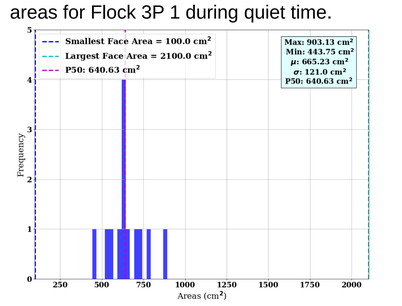

Figure 9: Flock 3P 1 optimized areas during quiet time assembled into a histogram.

RESULTS

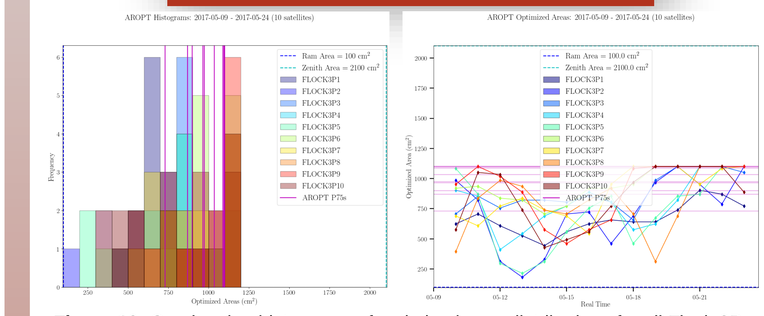

Figure 10: Overlapping histograms of optimized area distributions for all Flock 3P satellites (left) and their corresponding optimized areas over time (right)..

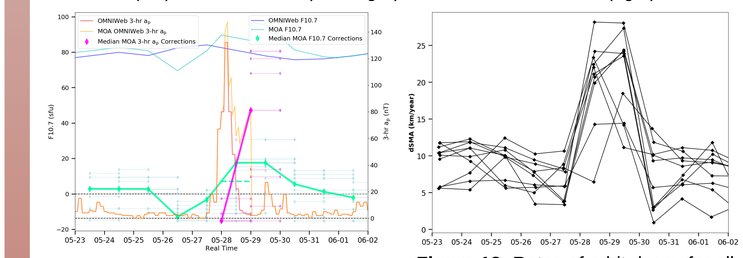

Figure 11: Linearly-interpolated F10.7 and Ap corrections for all satellites.

Figure 12: Rates of orbit decay for all satellites.

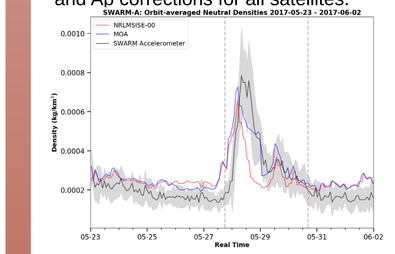

Figure 13: Corrected densities along-track SWARM-A.

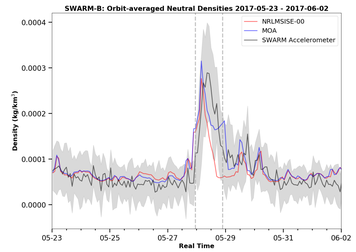

Figure 14: Corrected densities along-track SWARM-B.

DISCUSSION AND FUTURE WORK

- Density correction allowing for reductions up to 10% error in magnitude, on par with results obtained by Doornbos et al. 2008.
- Peak density width improved over NLRMSISE-00.
- Corrected densities more accurate than NLRMSISE-00 during initial onset.
- Corrected densities slightly too high right after storm main phase.
- Must validate the algorithm in other storms of varying intensities and using a variety of other calibration targets.
- Update MOA to incorporate F10.7 and a_p predictions for density forecasting.

REFERENCES

1. Kim, K.-H., et al., Atmospheric drag effects on the KOMPSAT-1 satellite during geomagnetic superstorms, *Earth Planets Space*, **58**, e25-28, 2006.
2. Bowman, B. R. and Storz, M. F., High accuracy satellite drag model (HASDM) review, *Space Environment Technologies – JB2008*, **AA3 03-625**, 2003.
3. Picone, J. M.; Hedin, A. E.; Drob, D. P.; Aikin, A. C. (2002-12-01). "NRLMSISE-00 empirical model of the atmosphere: Statistical comparisons and scientific issues". *Journal of Geophysical Research: Space Physics*, **107** (A12): 1468
4. Bussy-Virat, C. D., et al., The Spacecraft Orbital Characterization Kit and its Applications to the CYGNSS Mission, *2018 Space Flight Mechanics Meeting*, AIAA SciTech Forum, **AIAA 2018-1973**, 2018.
5. Storz, M. F., et al., High accuracy satellite drag model (HASDM), *Adv. Sp. Res.*, **36**, 12, pp. 2497-2505, 2005.
6. Doornbos et al., Use of two-line element set data for the thermosphere neutral density model calibration, *Adv. Sp. Res.*, **41**, pp. 1115-1122, 2008..

ACKNOWLEDGEMENTS

This research is support by NRL Grant Number N00173-18-1-G006 and a 2019 Michigan Space Grant Consortium Fellowship (Grant Number NNX15AJ20H).